Effects of steps and ordered defects on Cu(110) surface states

P. D. Lane,[1,*] D. S. Martin,[2] D. Hesp,[2] G. E. Isted,[1] and R. J. Cole[1]

[1]*SUPA, School of Physics and Astronomy, The University of Edinburgh, Edinburgh EH9 3JZ, United Kingdom*

[2]*Department of Physics and Surface Science Research Centre, The University of Liverpool, Liverpool L69 7ZE, United Kingdom*

(Received 28 September 2012; published 4 June 2013)

The effects of steps and ordered defects on the surface states supported by Cu(110) terraces are investigated by a combination of reflection anisotropy spectroscopy (RAS) and scanning tunneling microscopy (STM). For several vicinal (110)-type surfaces, we measure the 2.1-eV RAS peak arising from transitions between surface states. A Poelsema-Comsa scattering model is used to relate the intensity of this RAS signal to the surface morphology (the distributions of terrace widths and step-edge roughness) observed by STM, providing a measure of the ability of the surface defects to scatter the Shockley-type surface state. A scattering cross section of area equivalent to 20 unit cells is obtained—a value consistent with previous results obtained from other types of defect for the Cu(110) surface. We find that the Poelsema-Comsa scattering model, originally developed for random distributions of defects, is also applicable to the modeling of RAS intensities of surfaces with ordered and partially ordered defects: specifically steps. Our results highlight the growing importance of the Poelsema-Comsa methodology in combination with RAS data for extracting topographic information associated with surface defects, particularly from surfaces in hostile environments, where RAS can access as a real-time *in situ* probe.

DOI: 10.1103/PhysRevB.87.245405 PACS number(s): 78.68.+m, 78.40.−q, 73.20.At, 68.37.Ef

I. INTRODUCTION

Vicinal surfaces offer an attractive route into tailoring the morphology and electronic structure of solid interfaces. Created by introducing a specific miscut to a low-index single-crystal surface, a vicinal surface exhibits a "staircase" morphology of narrow terraces and a regular spatial arrangement of atomic steps.[1] In principle, vicinal surfaces allow the selection of terrace size, step direction, and step density. The differing coordination numbers of atoms at step edges creates reactive sites that are crucial in processes such as adsorption, surface functionalization, catalysis, and the growth of nanostructures, including one-dimensional atomic wires.[2,3] An ability to select terrace widths is important for controlling the spatial extent of molecular arrays, magnetic domains, and electronic surface states.[2] Scanning tunneling microscopy (STM) and optical techniques, in particular, reflection anisotropy (RA) spectroscopy (RAS), are well suited to the interrogation of these systems in both clean ultrahigh vacuum (UHV) conditions and in aqueous environments. Indeed, evidence from electrochemical-RAS experiments for the existence of surface states in aqueous environments has recently been reported.[4] In the work presented here, we investigate several vicinal surfaces with RAS and STM in order to isolate the effects of terrace width and step-edge roughness on the surface electronic states associated with Cu(110) terraces.

RAS,[5] also known as reflection difference spectroscopy, is a surface-sensitive optical technique that has been used to investigate atomic steps,[6–9] changes in surface symmetry,[10–12] and the behavior of surface states on metal surfaces.[13–26] RAS measures the difference in reflectivity between two orthogonal directions normalized to their average. Despite sensitivity to a range of surface phenomena, the interpretation of RA spectra is nontrivial; in recent years there have been attempts to obtain quantitative information from RA data, a number of which have focused on the 2.1-eV feature of Cu(110).[25,26] This feature arises primarily from transitions between two surface bands that lie on either side of the Fermi energy (E_F) in the *p-s* band gap at the $\bar{Y}$ point of the surface Brillouin zone. Photoemission spectroscopy results reveal that the occupied state lies ∼0.4 eV below E_F,[27–29] while inverse photoemission spectroscopy indicates that the unoccupied state lies ∼1.8 eV above E_F.[30–33] Optical RAS transitions between the two surface states require light polarized along the [001] direction,[34] producing anisotropy in the surface optical properties. The 2.1-eV feature has been found to be particularly sensitive to surface defects: thermally created defects,[25] defects created by ion bombardment,[25,26] and sensitivity to molecular adsorbates.[35–40]

Recently, attempts have been made to model the sensitivity of the RAS surface state intensity to surface defect distribution using the Poelsema-Cosma method.[41] Originally devised for He scattering, this method was first applied to RAS data by Sun *et al.*[19] in their study of CO adsorption onto Cu(110). Within this geometric scattering model, the signal of interest, I, is assumed to be destroyed over an area Σ surrounding each atomic defect. Equivalently, a surface site may be thought to contribute to I only if no defects fall within the area Σ surrounding that site. Since surface defects may have a footprint Σ larger than their physical size, the "active surface fraction," f_a, (and therefore I) need not follow the fraction of clean surface, $f_c = 1 - \Theta$. For example a surface with defect coverage Θ arranged as a lattice gas has a normalized signal given by

$$I = f_a(\Theta) = (1 - \Theta)^{n\Sigma}. \quad (1)$$

Here n is the surface atomic density, meaning that $n\Sigma$ is an effective scattering cross section measured in unit cells. Experimental RAS data from surfaces with adatoms and vacancies[24–26] and molecular adsorbates[19,25] have been found to be consistent with this expression with $n\Sigma \sim 20$. Furthermore, application of the Poelsema-Comsa model to the pseudorandom defect distribution produced by ion irradiation lead to very similar conclusions,[25] provided the clustering of adatoms around a vacancy island at each randomly distributed ion impact site was taken into account. Scanning tunneling

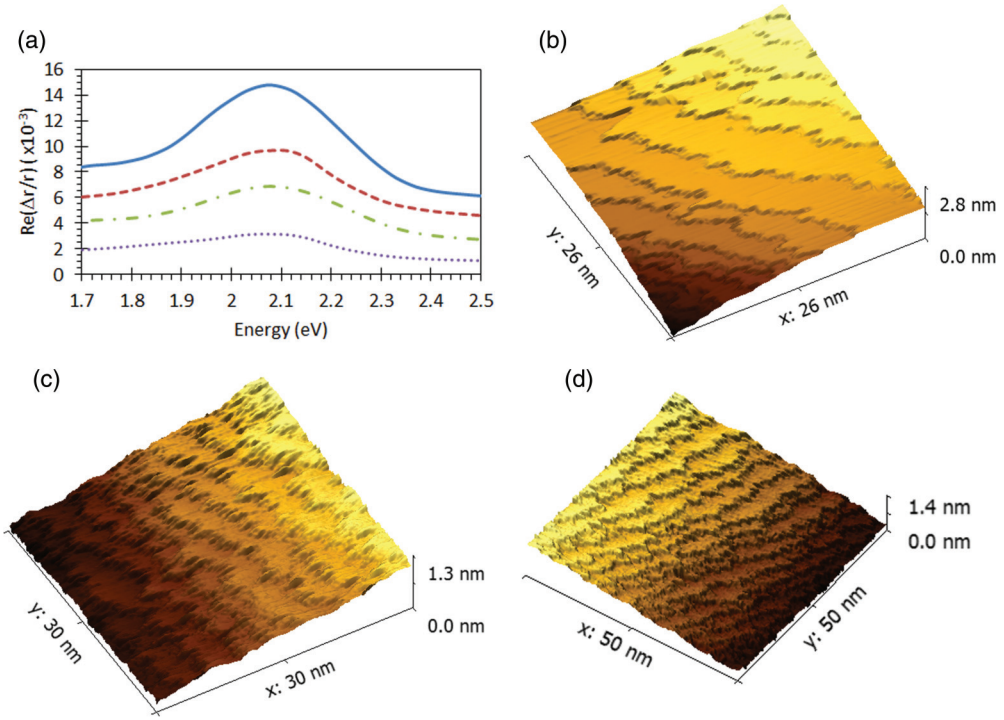

FIG. 1. (Color online) (a) The RA spectra of the Cu(110) surface (solid line), the Cu(10,9,0) surface (dashed line), the Cu(13,13,1) surface (dashed-dotted line), and the Cu(771) surface (dotted line). Also shown are STM images of (b) Cu(771) showing an area exhibiting large terraces, (c) Cu(13,13,1), and (d) Cu(10,9,0).

spectroscopy studies have shown that the local density of states around steps is completely quenched over a similar area (>1 nm^2) to Σ for defects or adsorbates.[42] Encouraged by this similarity, the present work investigates the applicability of the Poelsema-Comsa scattering model to the modeling of RAS intensities of surfaces with *ordered* defects: specifically steps. A complete description of disordered and ordered defects will advance the interpretation of RAS data and further develop its use as a real time *in situ* probe of optical and electronic structure at surfaces in environments in which other techniques such as STM and photoemission spectroscopy cannot easily access.

II. EXPERIMENT

Experiments were performed in a UHV environment with a base pressure in the region of 10^{-10} mbar. Clean Cu(110), Cu(771), Cu(13,13,1), and Cu(10,9,0) crystals were prepared by cycles of ion bombardment (500 eV, 300 K, 1.5 μA$\cdot$cm$^{-2}\cdot$s^{-1}, and 20 min) and annealing to 840 K. Surface order was confirmed by low-energy electron diffraction. RAS measurements were carried out on the standard phase modulated spectrometer of Aspnes design.[43]

The vicinal surfaces were chosen so that they all exhibit terraces of (110) orientation but of differing widths and bound by either [001] or [110] steps. In the cases of Cu(771) and Cu(13,13,1) the steps run parallel to the [110] direction, and the Cu(10,9,0) surface has steps that run parallel to the [001] direction. The perfect Cu(771) surface has terraces of a four-atom width, the perfect Cu(13,13,1) surface has seven-atom terraces, and the perfect Cu(10,9,0) surface has ten-atom terraces. The step density of the (110) surface and statistical data for the actual terrace widths of the vicinal surfaces were determined using room-temperature STM.

STM was performed in constant current mode using an Omicron STM. The tunneling current and bias voltage ranged between 0.5 to 1.0 nA and 1 to 2 V, respectively. STM tips were made from electrochemically etched tungsten wire. Image analysis, including measurements of terrace widths and step-edge roughness, was performed using Image SXM[44] and Gwyddion.[45] In order to determine an accurate value for the terrace widths to take into account the inhomogeneous nature of the terrace widths, the recorded width of a given terrace is an averaged value of multiple measurements taken at different positions across the length of the terrace.

The RA spectra of the clean Cu(110), Cu(771), Cu(13,13,1), and Cu(10,9,0) surfaces are shown in Fig. 1(a). All the surfaces show a positive peak at 2.1 eV whose intensity decreases as the step density increases. We will compare the intensities of the 2.1-eV RAS feature of the (110) terraces associated with these vicinal surfaces; by intensity, we mean the integrated area underneath the peak.

III. RAS SIMULATIONS OF VICINAL SURFACES

We now model the RAS signal of the vicinal surfaces by applying the Poelsema-Comsa algorithm to structures realized using the "solid-on-solid" model.[46] As explained in Sec. I, the normalized RAS signal is assumed to be given by the active surface fraction, f_a, which can be determined by considering a square "scattering patch" surrounding each lattice site in turn. Only if that patch contains no defects (adatoms or vacancies) will that site contribute to f_a.

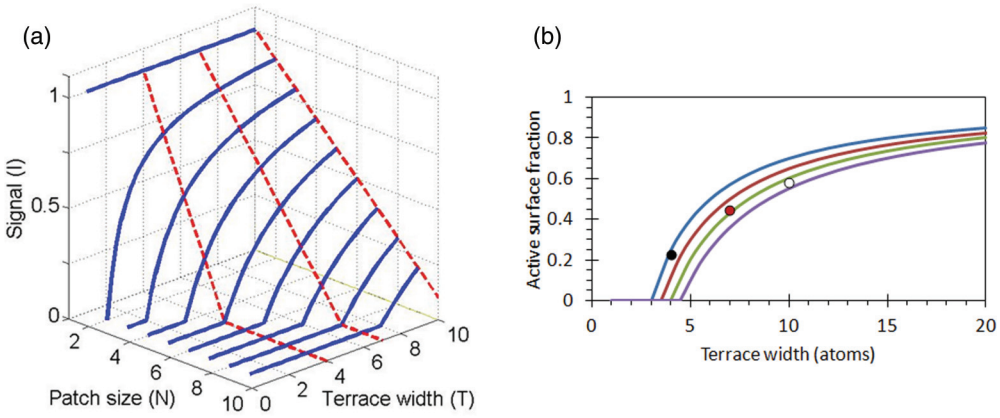

FIG. 2. (Color online) (a) Variation of the active surface fraction with terrace width, T, and patch size, N for perfect vicinal surfaces. Red lines show $I(N)$ for $T = 4$, 7, and 10. Blue lines show $I(T)$ for $N = 1, 2, \ldots 9$. (b) Symbols indicate the experimental RAS intensities of the Cu(771) surface (black circle), the Cu(13,13,1) surface (red circle), and the Cu(10,9,0) surface (white circle) normalized to that of the Cu(110) surface, plotted against the ideal terrace width. Solid curves show active surface fraction vs T calculated using Eq. (2) for $N = 4.0$, 4.5, 5.0, and 5.5.

A. Perfect surfaces

We define the perfect surface as one whose steps are smooth and parallel and whose terraces are of uniform width defined by their Miller indices. Upon applying square patches of side $N = \sqrt{n\Sigma}$ to each site of such a surface, it is seen that $(N-1)/2$ atoms at each end of the terrace do not contribute to the signal I. Where the terrace width, T, is less than the cutoff point $N-1$, the surface is rendered completely inactive, i.e., $I = f_a = 0$. For perfect surfaces with $T \geqslant N-1$, the normalized RAS signal is given by

$$I = f_a(N,T) = 1 - \left(\frac{N-1}{T}\right). \tag{2}$$

Figure 2(a) illustrates the dependence of I on patch size and terrace width. The red lines show the variation of I with N for three values of T relevant to the vicinal surfaces studied experimentally. As we consider larger patch sizes, less of the vicinal surface is active, with the effect seen more quickly for the shorter terrace surfaces. Similarly, the blue curves illustrate the predicted dependence of I on terrace width for a series of values of N. Interpretation of experimental RAS intensities using a perfect surface model for our vicinal samples is illustrated in Fig. 2(b). The Cu(110) surface is assumed to have an active surface fraction of 1.0, allowing normalization of the vicinal RAS signals. Although good agreement is not achieved, comparison with the simulated curves in Fig. 2(b) is broadly consistent with $N \sim 5$, equivalent to a scattering cross section of $n\Sigma \sim 25$. This value is consistent with previous work[24–26] that has yielded $3.5 \leqslant N \leqslant 6$ for a variety of adsorbates and surface defects on the Cu(110) surface. However, the STM results presented in Figs. 1(b)–1(d) reveal the perfect surface analysis to be naive in several respects. In particular, the average terrace widths depart from the ideal values deduced from the supposed Miller indices, nonuniformity in terrace widths is observed, as well as nonsmooth step edges. Statistical information on terrace width and roughness was extracted from such images for all four samples and is summarized in Table I.

We now use simulations to explore the consequence of these two effects on the active surface fraction.

B. Imperfect surfaces

To account for terrace width distributions, we can modify Eq. (2); thus,

$$I = f_a(N,\bar{T}) = \sum_{T \geqslant N-1} w_T^{\bar{T}} \left[1 - \left(\frac{N-1}{T}\right)\right]. \tag{3}$$

Here, $w_T^{\bar{T}}$ is the fraction of the surface made up of terraces of width T for a surface with average terrace width $\bar{T}$. Simulations using Eq. (3) and the "reasonable" value of $N = 5$ are shown in Fig. 3(a). The dashed red curve, calculated using a Poisson distribution for $w_T^{\bar{T}}$, shows the expected smoothing of the f_a vs $\bar{T}$ curve, as even surfaces with $\bar{T} < N-1$ now possess some active terraces, $\bar{T}$. Table I shows that the standard deviation in T is approximately 5 for the vicinal surfaces. The effect on active surface fraction of a Gaussian $w_T^{\bar{T}}$, with a standard deviation of 5 for all $\bar{T}$ is shown by the dot-dashed green curve in Fig. 3(a).

C. Step-edge roughness

"Frizzy" steps can be seen in Figs. 1(b)–1(d), and these will reduce the RAS signal more effectively than straight steps. We investigated this effect numerically using a terrace 1000 atoms

TABLE I. Model parameters determined by STM for the experimental samples studied.

	Terrace width			
Surface	Ideal	Measured	Standard deviation	Estimated step-edge roughness
(771)	4	6.0	6.4	0.2
(13,13,1)	7	9.1	4.3	0.3
(10,9,0)	10	14.5	5.1	0.2
(110)	—	60	71	0.2

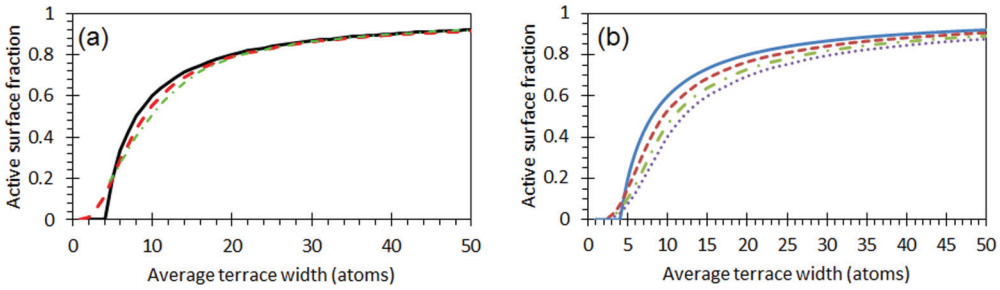

FIG. 3. (Color online) (a) Active surface fraction as a function of average terrace width for perfect vicinal surfaces (black solid line), surfaces with a Poisson distribution of terrace widths (red dashed curve), and surfaces with a Gaussian distribution of widths with standard deviation of 5 (green dotted-dashed curve). (b) Active surface fraction against average terrace width for rough step edges, where $R = 0$ (solid line), $R = 0.2$ (dashed line), $R = 0.5$ (dashed-dotted line), and $R = 1.0$ (dotted line). In all cases, a patch size of $N = 5$ has been assumed.

in length by an average width $\bar{T}$. The terrace was bounded by two rough steps initially $\bar{T}$ atoms apart, and the roughness was simulated by allowing the step position to vary by adding either -1, 0, or $+1$ to the previous position (meaning the terrace width would vary by between -2 and $+2$ atoms from site to site). We define step-edge roughness as the probability of the step position varying by ± 1 as we move in the direction parallel to the step edge. We ran Monte Carlo simulations for different roughness values and different average terrace widths to determine the effect of roughness on the active surface fraction. Results are shown in Fig. 3(b). We see that edge roughness shifts the cutoff edge of the f_a curve to higher $\bar{T}$ and reduces its gradient. Overall, the effect is similar to increasing N.

D. Comparison with experimental results

The RAS intensity of the surface state transition from our Cu(110) surface [Fig. 1(a)] is comparable to the values reported in previous studies,[13,21,25,26,35–40] so it should provide a valid normalization for the RAS peak intensities of the stepped surfaces. Nevertheless, a wide range of terrace widths (5 to 170 nm) was observed on the (110) surface, with an average of $\bar{T} \sim 60$ atoms and a standard deviation of $\sigma_T \sim 71$ atoms. Step-edge roughness was estimated to be $\sim$0.2. It follows that the active surface fraction of the Cu(110) surface was slightly less than 1.0. Using the step-edge roughness and terrace width distribution determined by STM, the active surface fraction of the Cu(110) surface can be simulated for any chosen value of N, allowing true normalization of the RAS intensities of the vicinal samples. In this way, we obtained the renormalized experimental data shown in Fig. 4 for $4 \leqslant N \leqslant 6$.

Having achieved the correct experimental normalization, we now add step-edge roughness to the simulations using the approach described in Sec. III B (with a Gaussian distribution function of standard deviation of 5). An upper bound for the effect of step-edge roughness on active surface fraction was obtained using the method described in Sec. III C (with $R = 1$). Results are illustrated in Fig. 4. Using the appropriate combinations of step distributions and step-edge roughness, we obtain lower and upper bounds as to where we might expect the experimental data to lie (shaded region). Agreement between simulation and experiment is achieved for $5 \leqslant N \leqslant 6$, equivalent to a scattering cross section in the range $25 \leqslant n\Sigma \leqslant 36$. Correctly normalizing the experimental

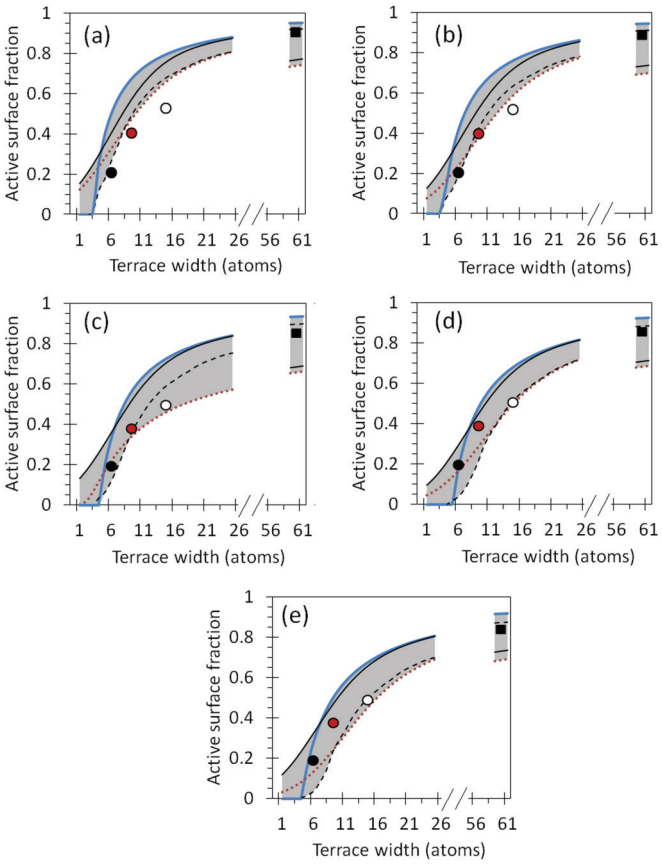

FIG. 4. (Color online) Calculated active surface fraction against terrace width for patch sizes (a) $N = 4$, (b) $N = 4.5$, (c) $N = 5$, (d) $N = 5.5$, and (e) $N = 6$. In each case, results are shown for simulations assuming perfect surfaces (thick solid blue line), uniform terrace widths with rough step edges (dashed black line), a distribution of terrace widths with straight step edges (solid black line), and a distribution of terrace widths with rough step edges (dotted red line). RAS intensities against STM terrace widths of the Cu(771) surface (black circle), Cu(13,13,1) surface (red circle), Cu(10,9,0) surface (white circle), and Cu(110) (filled square) are also represented. In the high T region, the terrace width distribution observed experimentally for the Cu(110) sample was used in the simulations. In the low T region, a Gaussian distribution with a standard deviation of 5 was used.

data and plotting it at the true $\bar{T}$ tend to increase estimates of N obtained by the naive procedure discussed in Sec. III A. Accounting for the imperfection of the vicinal surfaces gives a similar but slightly smaller shift in the opposite direction.

IV. DISCUSSION

This work only considers the effects of steps on the intensity of the 2.1-eV feature. We know defects can arise from other sources: on the clean surface, the effect of thermal defects[25] and on ion-bombarded surfaces by ion-induced defects,[26] these too could affect the intensity of the peak. For this work we consider only the clean surfaces with different step densities, so we can ignore the effects of ion bombardment; however, one could imagine that thermal defects could be present. Randomly distributing defects on these surfaces would to a first approximation reduce all the intensities by a similar amount. However, when considering the problem in more detail, it becomes apparent that the position of defect sites is important. Sites close to step edges have already had their contribution quenched, and adding an additional defect to these sites could have little or no effect on the signal measured, meaning that the addition of a given number of defects could show larger changes to the surface state intensity on surfaces with long terraces than on surfaces with short terraces. This problem could be complicated further as the higher step density could be both a source of additional defects from the steps and a sink for defects diffusing from the terrace.

Similar to the (110) surfaces, the terraces of the Cu, Au, and Ag(111) surfaces support Shockley-type surface states. These states are also present on vicinal (111) noble metal surfaces and are known to be sensitive to the effects of lateral confinement resulting from the vicinal surface morphology.[47–50] Regular arrays of monoatomic steps terminating narrow terraces result in a partial confinement of the surface state and a shift towards E_F in the binding energy of the state. The magnitude of the shift towards E_F is inversely proportional to the square of the terrace width. For two vicinal Cu(111) surfaces whose terraces are of width 12 and 15 Å (15 Å is seven atoms), shifts in binding energy of 45 and 80 meV, respectively, are observed in photoemission results.[48] The binding energy of the state on the flat Cu(111) surface is 0.39 eV. In addition to the energy shift, the intensities of photoemission peaks observed from confined states are lower with a broader line shape than that observed from the flat (111) surface.[48] The RA results of the vicinal (110) surfaces studied here show changes in the intensity of the 2.1-eV feature [Fig. 1(a)]; however, these changes are much larger than the confinement effects, and no shift in peak energy is observed. Thus, either no such effects are present for our vicinal surfaces, or the effects are not observable with RAS. The vicinal (111) surfaces have a relatively high degree of terrace width uniformity and step-edge smoothness,[48] which is not the case for our room-temperature surfaces [Figs. 1(b)–1(d)]. We suggest that this loss of periodicity is likely to diminish any confinement effects.

The study by Martin *et al.* of the ion bombardment of a stepped Cu(110) surface[22] provides both some justification of the results in this work and the problems caused by the energetics of such systems. The stepped surface in Ref. 22 has narrow, uniform width terraces with relatively smooth step edges, and no surface state RAS feature is observed. The confinement effect was suggested to explain the absence of the 2.1-eV RAS peak for the stepped Cu(110) surface.[22] As the stepped surface is bombarded by ions, the terrace width increases, the intensity of the surface state peak was found to increase, and continued ion bombardment sees the peak intensity start to reduce again. This work and previous studies have allowed the effects of surface defects on the surface state to be described by a simple geometric model.[24–26] These models would offer a method of calibrating molecular dynamics or kinetic Monte Carlo methods for studying time-evolving processes such as behavior of stepped surfaces undergoing ion bombardment.[22] A recent study[51] has shown good agreement between molecular dynamics simulations and experimental studies of ion damage on the surface of Cu(110) and may provide a starting point for further work in this area.

V. CONCLUSIONS

We have considered the effects of steps and ordered defects on the Cu(110) surface terraces by applying a simple geometric model based on the principles of a model by Poelsema and Cosma[41] and applied to RAS data by Sun *et al.*[19] This model was initially developed for random distributions of defects. We apply the principles of a scattering cross section and patch size to a system of ordered defects. Through the use of experimental results and computer models, we have identified the importance of the size of the terraces and the roughness of the edges of the boundaries in relation to the patch size and how these parameters influence the surface state intensity. Using STM, we were able to obtain data about the distributions of terrace widths and estimate the step-edge roughness, which allowed us to determine a patch size $5 \leqslant N \leqslant 6$, which is consistent with values obtained from other arrangements and different types of defect. As more surface nanostructures are studied by the visible light-based RAS technique, we anticipate that the Poelsema-Comsa methodology will be widely employed, and its potential realized for extracting topographic information associated with surface defects, particularly from samples in hostile environments that are not accessible to electron-based techniques.

ACKNOWLEDGMENTS

The authors would like to thank B. Macdonald for recording the RAS measurements of the Cu(771) and Cu(10,9,0) surfaces and V. Dhanak for access to the STM facilities.

*Corresponding author: paul.lane@ed.ac.uk; Present address: School of Chemistry, The University of Edinburgh, Edinburgh, EH9 3JJ, United Kingdom.

[1] H.-C. Jeong and E. D. Williams, Surf. Sci. Rep. **34**, 171 (1999).
[2] A. Mugarza, F. Schiller, J. Kuntze, J. Cordon, M. Ruiz-Oses, and J. E. Ortega, J. Phys.: Condens. Matter **18**, S27 (2006).

[3]C. Tegenkamp, J. Phys.: Condens. Matter **21**, 013002 (2009).
[4]E. E. Barritt, C. I. Smith, D. S. Martin, K. Gentz, K. Wandelt, and P. Weightman, Europhys. Lett. **92**, 57005 (2010).
[5]P. Weightman, D. S. Martin, R. J. Cole, and T. Farrell, Rep. Prog. Phys. **68**, 1251 (2005).
[6]S. G. Jaloviar, J.-L. Lin, F. Liu, V. Zielasek, L. McCaughan, and M. G. Lagally, Phys. Rev. Lett. **82**, 791 (1999).
[7]W. G. Schmidt, F. Bechstedt, and J. Bernholc, Phys. Rev. B **63**, 045322 (2001).
[8]F. Baumberger, Th. Herrmann, A. Kara, S. Stolbov, N. Esser, T. S. Rahman, J. Osterwalder, W. Richter, and T. Greber, Phys. Rev. Lett. **90**, 177402 (2003).
[9]M. Schwitters, D. S. Martin, P. Unsworth, T. Farrell, J. E. Butler, M. Marsili, O. Pulci, and P. Weightman, Phys. Rev. B **83**, 085402 (2011).
[10]B. F. Macdonald and R. J. Cole, Appl. Phys. Lett. **80**, 3527 (2002).
[11]B. F. Macdonald, J. S. Law, and R. J. Cole, J. Appl. Phys. **93**, 3320 (2003).
[12]P. D. Lane, G. E. Isted, D. S. Roseburgh, and R. J. Cole, Appl. Phys. Lett. **95**, 141907 (2009).
[13]Ph. Hofmann, K. C. Rose, V. Fernandez, A. M. Bradshaw, and W. Richter, Phys. Rev. Lett. **75**, 2039 (1995).
[14]J.-K. Hansen, J. Bremer, and O. Hunderi, Surf. Sci. Lett. **418**, L58 (1998).
[15]K. Stahrenberg, Th. Herrmann, N. Esser, and W. Richter, Phys. Rev. B **61**, 3043 (2000).
[16]D. S. Martin, A. M. Davarpanah, S. D. Barrett, and P. Weightman, Phys. Rev. B **62**, 15417 (2000).
[17]D. S. Martin, O. Zeybek, B. Sheridan, S. D. Barrett, P. Weightman, J. E. Inglesfield, and S. Crampin, J. Phys.: Condens. Matter **13**, L1 (2001).
[18]D. S. Martin and P. Weightman, J. Phys.: Condens. Matter **14**, 675 (2002).
[19]L. D. Sun, M. Hohage, P. Zeppenfeld, R. E. Balderas-Navarro, and K. Hingerl, Phys. Rev. Lett. **90**, 106104 (2003).
[20]P. Monachesi and L. Chiodo, Phys. Rev. Lett. **93**, 116102 (2004).
[21]L. D. Sun, M. Hohage, P. Zeppenfeld, and R. E. Balderas-Navarro, Surf. Sci. **589**, 153 (2005).
[22]D. S. Martin, R. J. Cole, and P. Weightman, Phys. Rev. B **72**, 035408 (2005).
[23]D. S. Martin, J. Phys.: Condens. Matter **21**, 405003 (2009).
[24]G. E. Isted, P. D. Lane, and R. J. Cole, Phys. Rev. B **79**, 205424 (2009).
[25]P. D. Lane, G. E. Isted, and R. J. Cole, Phys. Rev. B **82**, 075416 (2010).
[26]G. E. Isted, P. D. Lane, R. J. Cole, M. Caffio, and R. Schaub, Phys. Rev. B **83**, 155403 (2011).
[27]P. Heimann, J. Hermanson, H. Miosga, and H. Neddermeyer, Surf. Sci. **85**, 260 (1979).
[28]S. Kevan, Phys. Rev. B **28**, 4822 (1983).
[29]P. Straube, F. Pforte, T. Michalke, K. Berge, A. Gerlach, and A. Goldmann, Phys. Rev. B **61**, 14072 (2000).
[30]R. A. Bartynski, T. Gustafsson, and P. Soven, Phys. Rev. B **31**, 4745 (1985).
[31]B. Reihl and K. H. Frank, Phys. Rev. B **31**, 8282 (1985).
[32]R. Schneider, H. Durr, Th. Fauster, and V. Dose, Phys Rev. B **42**, 1638 (1990).
[33]D. Heskett, D. DePietro, G. Sabatino, and M. Tammarro, Surf. Sci. **513**, 405 (2002).
[34]M. Y. Jiang, G. Pajer, and E. Burstein, Surf. Sci **242**, 306 (1991).
[35]B. G. Frederick, J. R. Power, R. J. Cole, C. C. Perry, Q. Chen, S. Haq, Th. Bertrams, N. V. Richardson, and P. Weightman, Phys. Rev. Lett. **80**, 4490 (1998).
[36]R. J. Cole, B. G. Frederick, J. R. Power, C. C. Perry, Q. Chen, C. Verdozzi, N. V. Richardson, and P. Weightman, Phys. Status Solidi A **170**, 235 (1998).
[37]C. C. Perry, B. G. Frederick, J. R. Power, R. J. Cole, S. Haq, Q. Chen, N. V. Richardson, and P. Weightman, Surf. Sci. **427**, 446 (1999).
[38]D. S. Martin, R. J. Cole, and S. Haq, Phys. Rev. B **66**, 155427 (2002).
[39]L. D. Sun, R. Denk, M. Hohage, and P. Zeppenfeld, Surf. Sci. **602**, L1 (2008).
[40]D. S. Martin, P. D. Lane, G. E. Isted, R. J. Cole, and N. P. Blanchard, Phys. Rev. B **82**, 075428 (2010).
[41]B. Poelsema and G. Cosma, *Scattering of Thermal Energy Atoms* (Springer, Berlin, 1989), Vol. 115.
[42]Ph. Avouris, I.-W. Lyo, and P. Molinàs-Mata, Chem. Phys. Lett. **240**, 423 (1995).
[43]D. E. Aspnes, J. P. Harbison, A. A. Studna, and L. T. Florez, J. Vac. Sci. Technol. A **6**, 1327 (1988).
[44]Image SXM, http://www.ImageSXM.org.uk (accessed on 2nd March 2012).
[45]D. Nečas and P. Klapetek, Cent. Eur. J. Phys. **10**, 181 (2012); Gwyddion, http://gwyddion.net/ (accessed on 2nd March 2012).
[46]See, for example, G. A. Somorjai, *Chemistry in Two Dimensions: Surfaces* (Cornell University Press, Ithaca, New York, 1981).
[47]L. C. Davis, M. P. Everson, R. C. Jaklevic, and Weidian Shen, Phys. Rev. B **43**, 3821 (1991).
[48]O. Sanchez, J. M. Garcia, P. Segovia, J. Alvarez, A. L. Vazquez de Parga, J. E. Ortega, M. Prietsch, and R. Miranda, Phys. Rev. B **52**, 7894 (1995).
[49]A. Mugarza and J. E. Ortega, J. Phys.: Condens. Matter **15**, S3281 (2003).
[50]M. Hansmann, J. I. Pascual, G. Ceballos, H.-P. Rust, and K. Horn, Phys. Rev. B **67**, 121409(R) (2003).
[51]P. D. Lane, G. J. Galloway, R. J. Cole, M. Caffio, R. Schaub, and G. J. Ackland, Phys. Rev. B **85**, 094111 (2012).